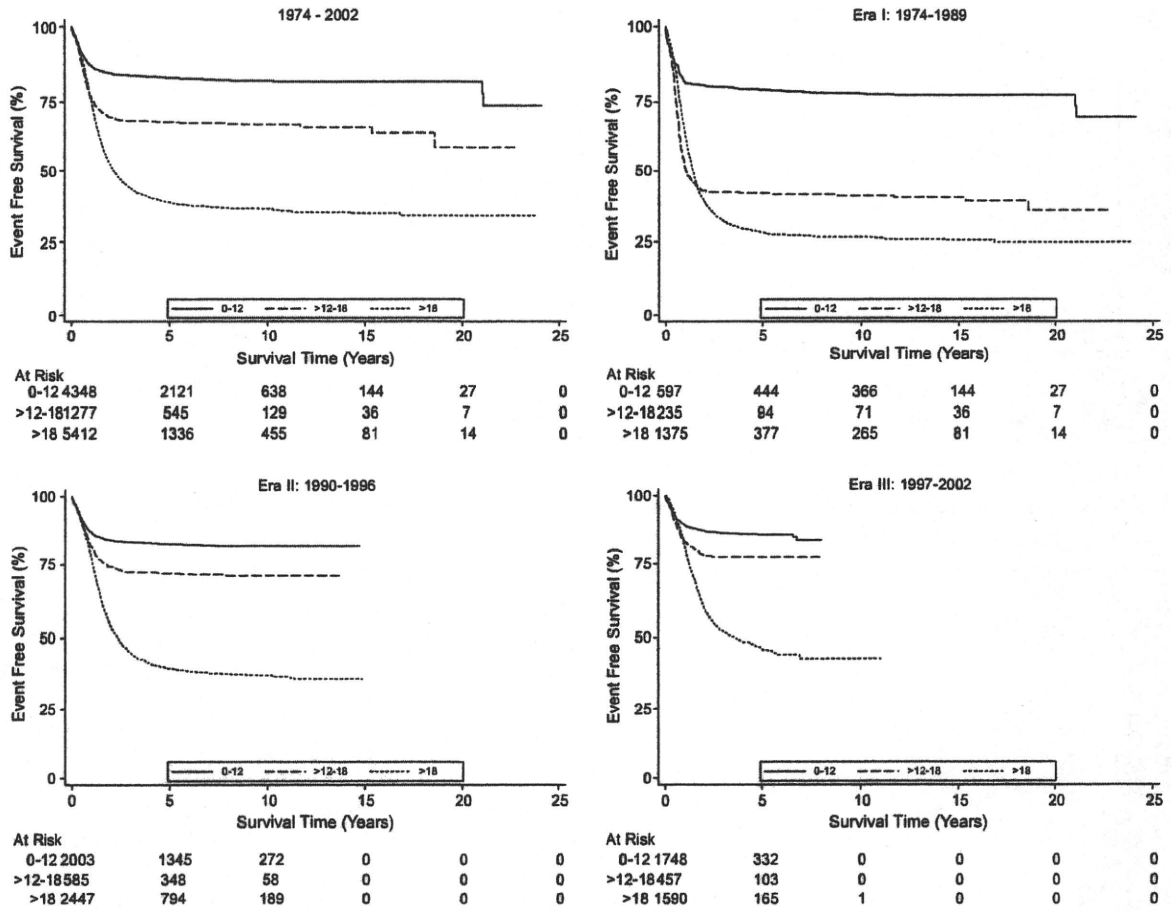

Fig. 3 – EFS for all 11,037 patients, and within each Era, for the age categories 0–12, 13–18 and 19 or more months.

in a decrease in the risk associated with *MYCN* amplification compared to the risk if *MYCN* is considered alone. However, amplification remains adversely prognostic in Era III (HR 2.62: 2.35–3.04, $p < 0.001$).

An alternative approach to assessing outcome is to assign a weight of −1, 0, or 1 to each risk factor (age-at-diagnosis, BM metastases, *MYCN* status), where the weight corresponds to the low-, intermediate- and high-risk categories. Using the weights, analyses determined that each risk factor exerted approximately the same level of prognostic influence on outcome (results not shown). On this basis, all possible combinations of low-, intermediate-, or high-risk of age, BM metastases and *MYCN* status create different groups. For each patient, the weights are summed to a score and those with the same score are combined into groups. For example, the weights for patients age-at-diagnosis 0–12 (weight: −1), unknown BM status (0) and amplified *MYCN* (1) sum to 0 (zero). These patients would be combined with others who have a sum of 0, for example, those aged 19+ months (weight: 1), with no BM metastases (−1), and unknown *MYCN* (0). This process results in seven groups with scores ranging from −3 (all factors indicating low-risk) to +3 (high-risk) but then coded 0–6 for convenience. The corresponding EFS curves indicate a worsening prognosis with increasing score, within each era as well as over the entire period (Fig. 6). On this basis, visual inspection of the EFS curves of Era III suggests a possibility of four major risk categories with scores (0, 1), (2), (3), and (4, 5, 6), respectively. This underlines the fact that, despite the considerable improvement in the overall prognosis of young patients with NB, major outcome differences remain.

4. Discussion

The International Neuroblastoma Risk Group (INRG) Task Force collated, after extensive consultation and international collaboration, data from 11,037 patients with neuroblastoma (NB) in those less than 21 years of age-at-diagnosis and recruited to clinical studies between 1974 and 2002. With these data INRG have proposed a revised classification system based on the 8800 patients diagnosed between 1990 and 2002.[9,13] The objective of the revised classification was to identify risk groups, ranging from very-good to very-poor prognosis, to enable focus for devising better therapeutic strategies. It is hoped that this will accelerate the improvement in outcome achieved over previous decades for all patients of whatever risk category. A key consideration for this revised classification was whether the age-at-diagnosis cut-off of greater than 12 months should be revised as it had been suggested, from an analysis of 3666 patients, that this might be raised to those who are >18 months.[15] The further data

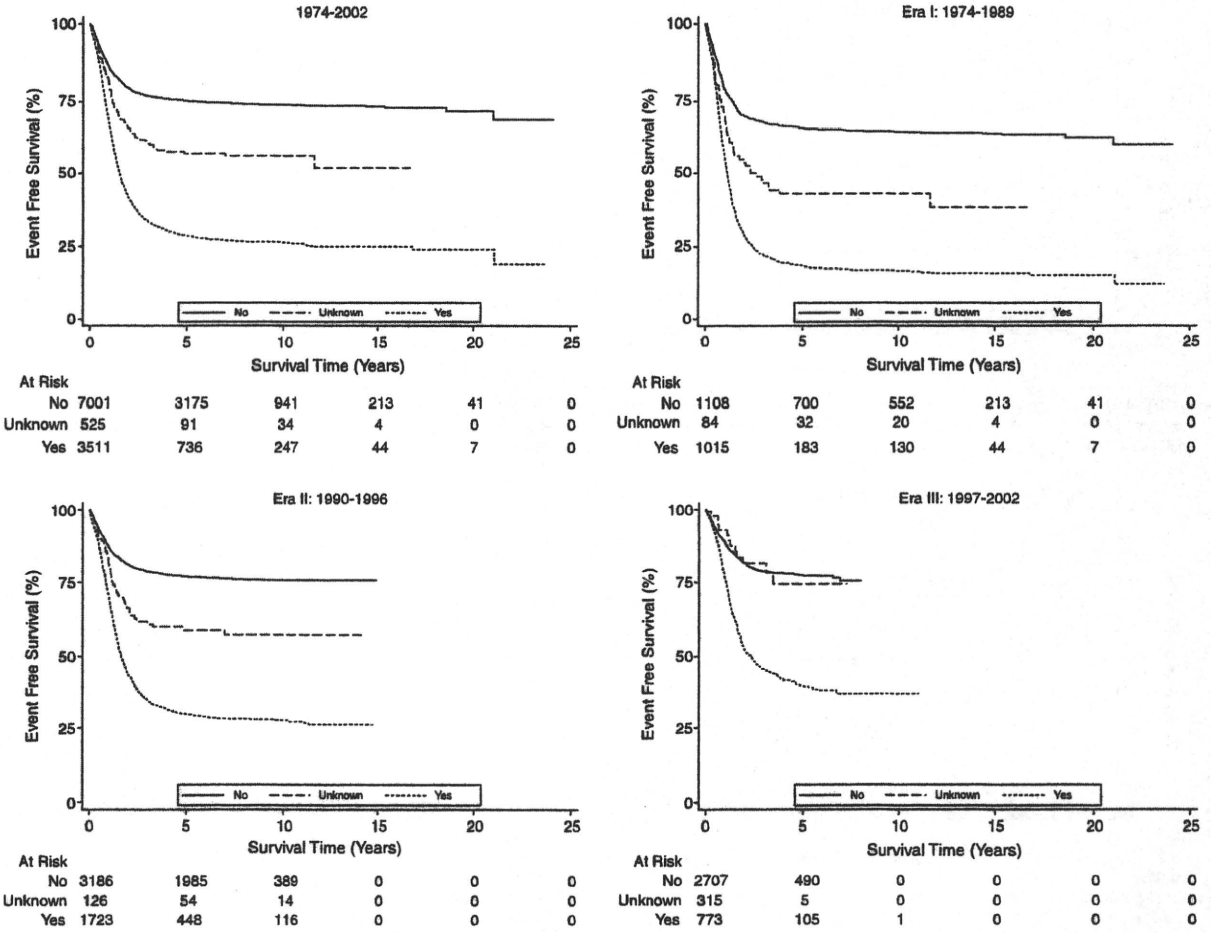

Fig. 4 – EFS for all 11,037 patients, and within each Era, for the three BM involvement groups.

available from 1990 to 2002 subset of the INRG database have demonstrated statistical and biological confirmation for the revision. Thus the INRG classification system regards those with age-at-diagnosis >18 months as at higher risk although this is only one of the seven criteria used to determine risk.

Many modifications in treatment and supportive care have occured over time: the three Era (1974–89; 1990–96 and 1997–2002) serve as a surrogate variable encapsulating all factors that have changed. The main focus of this study is to investigate whether the general prognosis for children with NB has improved over time and, in particular, to establish whether age-at-diagnosis still plays a major role in subsequent outcome. It is well established that other features recorded at diagnosis will also be important determinants but to investigate change over the full 28-year period we are constrained to variables that were recorded in the earlier times. This precluded, for example, detailed study of chromosome 11q status, and DNA ploidy but permitted investigation of *MYCN* status and the presence of metastatic disease in the bone marrow. Although stage is a well established clinical prognostic factor in NB, as age is used within the INSS procedure itself to define 4s disease, it could not be considered as a prognostic variable for the purposes of our analysis.

It is recognised that definitions, investigative methods, laboratory techniques and standards of recording are very likely to differ widely over the different international groups each collating information from many individual participating centres on the 11,037 patients concerned. It is also recognised that some subjectivity was utilised in choosing, for example, BM involvement rather than bone metastases for our model although each appeared to be similarly influential on outcome. The former was chosen on statistical grounds as having the fewer missing values, a more even spread in those with and without involvement, and a larger hazard ratio. Further, we were not attempting to develop a full prognostic model for use with future patients (this would need to consider the most recent items now available) but merely to give a broad description of the changes over the era and the influence of age-at-diagnosis using simple statistical models. In full recognition that a substantial part of the data (Era II and III) had been used in developing the INRG classification, we used an entirely different statistical approach, the proportional hazards regression model,[10] to substantiate or otherwise the age-at-diagnosis classification.

We show that the 3-year EFS increased from 46% for patients diagnosed from 1974–1989 to 63% for 1990–1996, to 71% for 1997–2002.

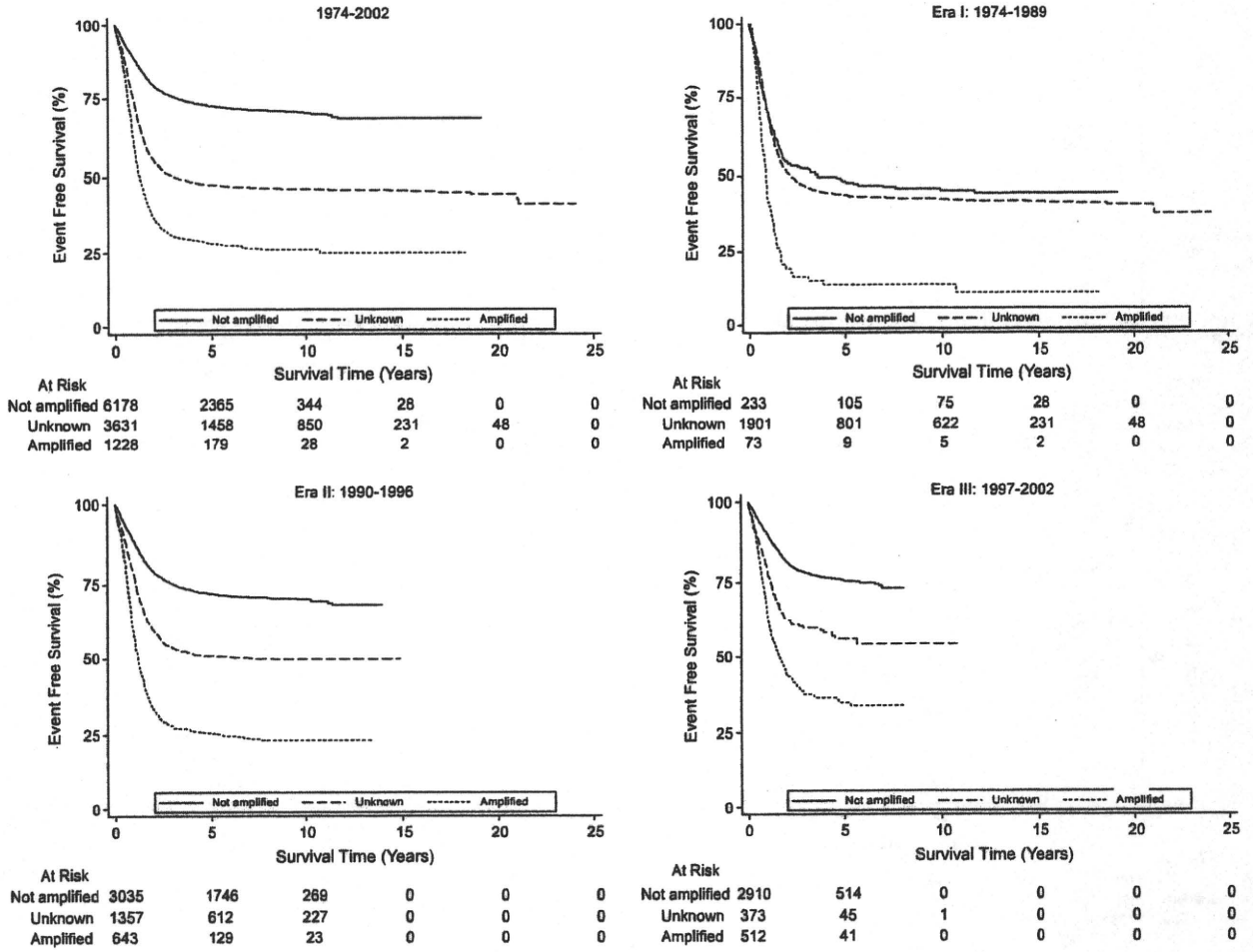

Fig. 5 – EFS for all 11,037 patients, and within each Era, for the MYCN amplification groups.

Table 3 – Multivariable estimates of HRs for EFS by age in 6 categories and evidence of BM disease and MYCN amplification for each of three era and all times. (Univariate HRs are indicated in parenthesis).

		n (%)	All events	Hazard ratio (HR)				EFS (%)	
				Era I 1974–1989	Era II 1990–1996	Era III 1997–2002	All era	3-year	5-year
Age (*m*)	–6	2441 (22)	384	1	1	1	1	84.11	83.51
	7–12	1907(17)	327	1.22	0.98	0.95	1.02	83.46	82.46
	13–15	703 (6)	187	3.03	1.00	1.42	1.47	72.43	72.24
	16–18	574 (5)	210	4.52	1.97	1.51	2.34	63.38	62.65
	19–24	925 (8)	412	3.29	2.10	2.09	2.39	53.92	52.06
	25+	4487 (41)	2746	3.57	2.68	2.83	2.95	41.16	35.62
	Univariate HR of 25+ group			(5.52)	(4.65)	(4.04)	(4.83)		
Bone marrow metastases	No	7001(63)	1665	1	1	1	1	77.00	75.36
	Unknown	525 (5)	109	1.64	1.65	1.05	1.25	60.97	56.99
	Yes	3511 (32)	2492	2.81	2.86	2.14	2.68	33.34	28.62
	Univariate HR of Yes group			(3.66)	(4.25)	(3.16)	(4.00)		
MYCN amplified	No	6178 (56)	1555	1	1	1	1	75.60	72.52
	Unknown	3631 (33)	1880	0.98	1.47	1.62	1.64	50.13	47.52
	Yes	1228 (11)	831	1.88	2.77	2.62	2.58	30.80	28.28
	Univariate HR of Yes group			(2.50)	(4.24)	(3.86)	(3.97)		
	Total	11037	4266	2207	5035	3795			

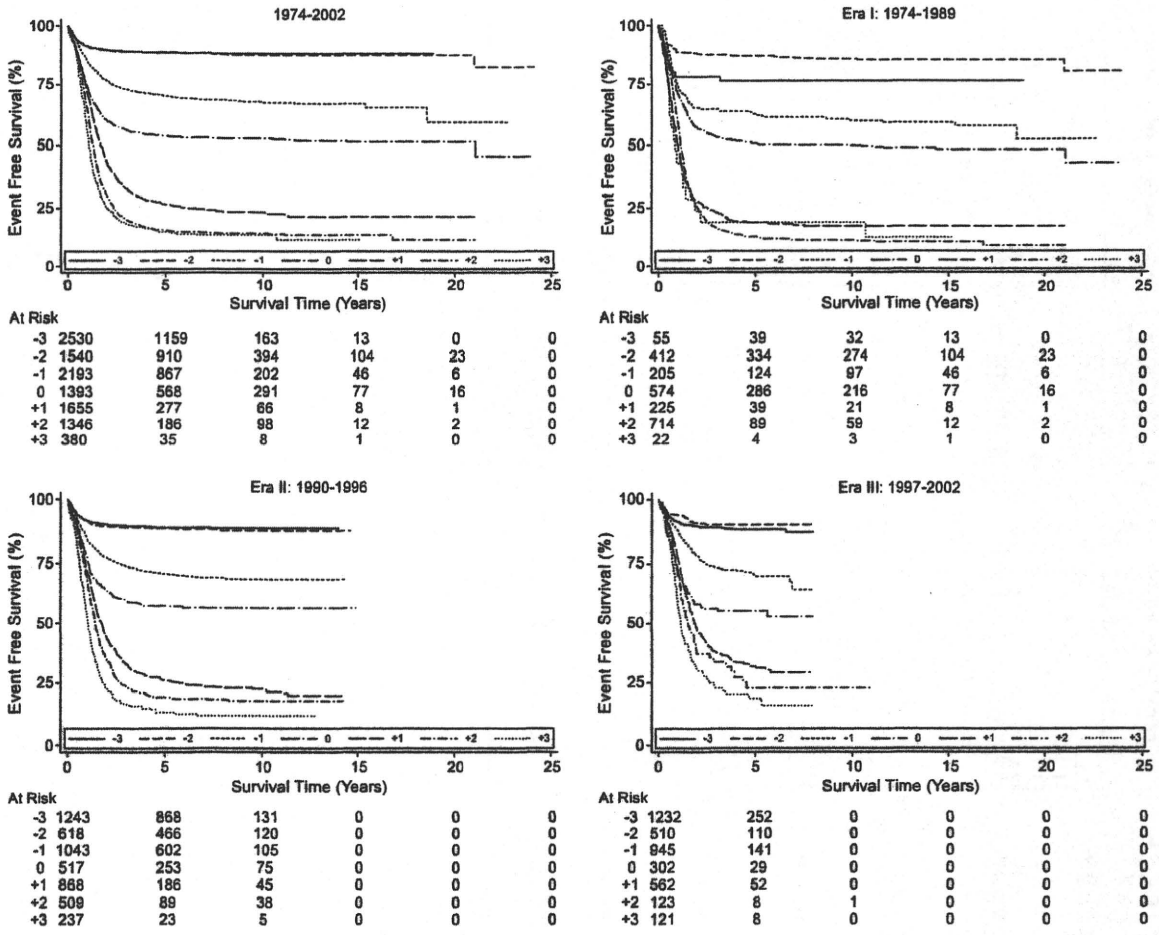

Fig. 6 – EFS for the seven risk groups defined by age-at-diagnosis (3 groups), together with the presence or absence of metastatic BM involvement and *MYCN* amplification.

Ignoring all other considerations, age-at-diagnosis appears to have retained an important role over the 28-year period. However, this influence is gradually waning over calendar time with, for example, those of >18 months having a 3-year EFS increasing from 25% in those diagnosed 1974–1989 to 45% in those from 1997–2002 (Fig. 3). Adjusting treatment in those over 12 months to compensate for their relatively poorer prognosis may have contributed to this. It also remains apparent (Table 2) that the risk of relapse increases steadily with age so that no single cut is likely to divide good and poor prognosis unambiguously for all. Thus, there remains some suggestion that those diagnosed between 13 and 18 months remain at higher risk than the youngest children, and that those >18 months are at an even greater risk of relapse. A pragmatic cut beyond 18 months for prognostic purposes for future patients does not seem unreasonable. It is important to note that wherever a cut is made, those close to this (convenient) boundary are at very similar risk. The increasing age risk remains the case, although diminished in magnitude, whether or not the presence or otherwise of metastases in the BM or *MYCN* oncogene status is taken into account. Although only future data can substantiate this, it is likely that strength of increasing age-at-diagnosis as an adverse prognostic variable will continue to decline.

For patients with high-risk disease, treatment strategies have been increasingly intensified over time. Further, the use of myeloablative therapy and stem cell transplants increased following the Children's Cancer Group randomized trial[16] and this too may have contributed to both the improved EFS and the decreasing influence of age-at-diagnosis.

Although older age, *MYCN* amplification and the presence of BM metastases were independently predictive of poor outcome, the unfavourable prognostic influence of either one of these is offset by the absence of one or more of the remaining unfavourable factors (Fig. 6).

It has been suggested that age-at-diagnosis may be a proxy for as undescribed tumour-related factor. However, it may be that some current prognostic features, such as *MYCN*-status, should be reconsidered but on a continuous scale rather than categorised (amplified, not amplified) as when considered in this way they may mimic more closely the situation that is apparent with age.

There is strong evidence that the strategy of increasing therapeutic intensity has improved the outcome for children with NB over the 1974–2002 period and that there is a declining influence of the prognostic effect of age-at-diagnosis. Nevertheless the strength of the three most powerful factors, *MYCN* status, BM metastases and age, remains high.

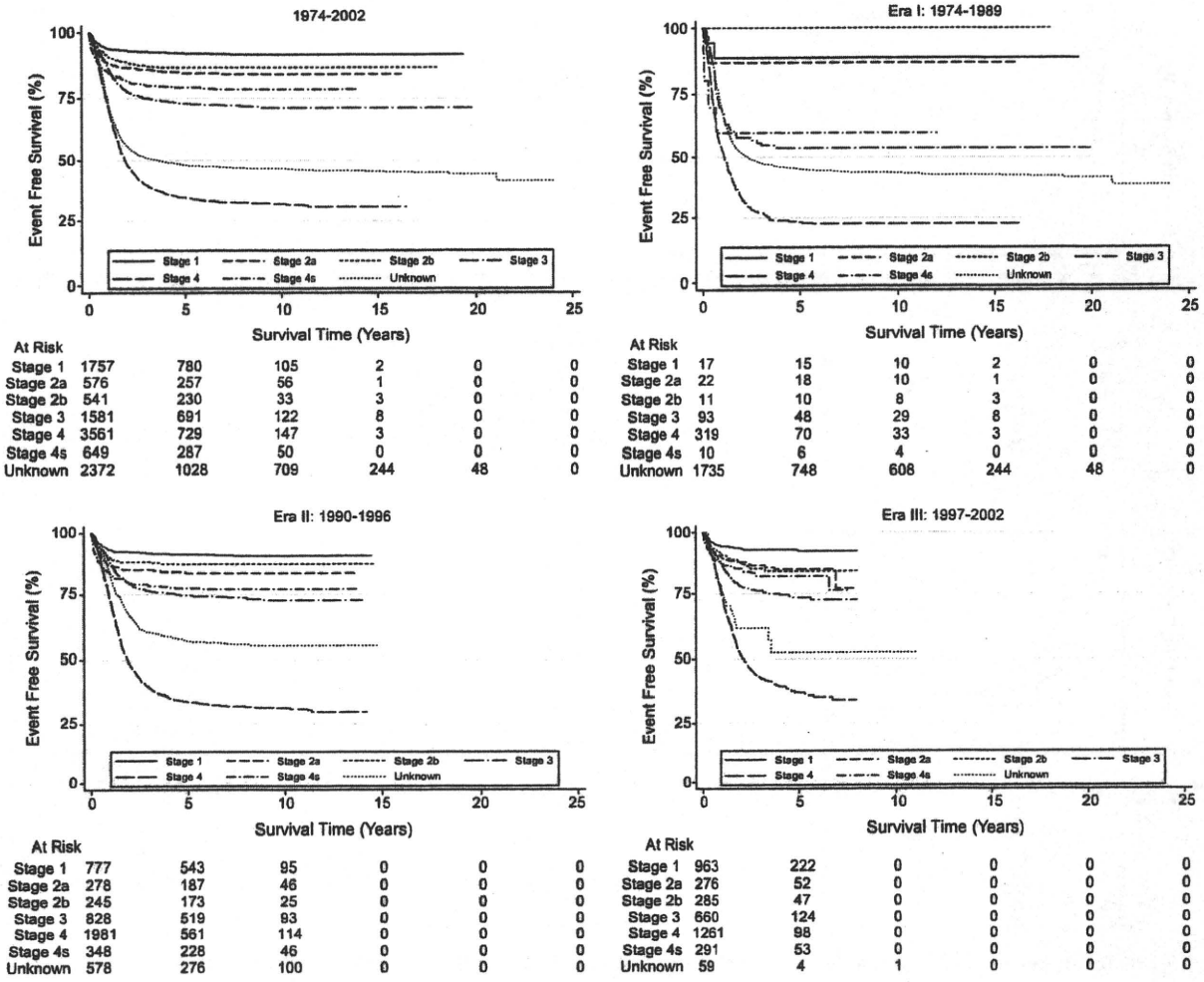

Fig. A1 – EFS for all 11,037 patients, and within each Era, for each INSS stage.

Conflict of interest statement

None declared.

Acknowledgements

Supported in part by the William Guy Forbeck Research Foundation, Little Heroes Pediatric Cancer Research Foundation, the Italian Neuroblastoma Foundation, the Italian Ministry of Health "Ricerca Finalizzata – Bando Oncologia 2006", NIH/NCI U10-CA98543 COG Group Chair's Grant, NIH/NCI U10-CA98413 COG member institution's grant and NIH/NCI U10-CA29139 and U10 CA98413 COG Statistics and Data Center grants. We thank all the collaborators and patients from centres in the following countries who have participated in the INRG project: Australia, Austria, Belgium, Canada, Denmark, France, Germany, Italy, Ireland, Japan, New Zealand, Norway, Spain, Sweden, Switzerland, UK and the USA.

Appendix A

See Fig. A1.

REFERENCES

1. Breslow N, McCann B. Statistical estimation of prognosis for children with neuroblastoma. *Cancer Res* 1971;31:2098–103.
2. Evans AE. Staging and treatment of neuroblastoma. *Cancer* 1980;45:1799–802.
3. Brodeur GM. Neuroblastoma: biological insights into a clinical enigma. *Nat Rev Cancer* 2003;3:203–16.
4. Cecchetto G, Mosseri V, De Bernardi B, et al. Surgical risk factors in primary surgery for localized neuroblastoma: the LNESG1 study of the European International Society of Pediatric Oncology Neuroblastoma Group. *J Clin Oncol* 2005;23:8483–9.
5. Kushner BH, Cohn SL. Intermediate-risk Neuroblastoma. In: Cheung N-KV, Cohn SL, editors. *Neuroblastoma*. Heidelberg: Springer-Verlag; 2005. p. 131–7.

6. Attiyeh EF, London WB, Mosse YP, et al. Chromosome 1p and 11q deletions and outcome in neuroblastoma. *N Engl J Med* 2005;**353**:2243–53.
7. Caron H, van Sluis P, de Kraker J, et al. Allelic loss of chromosome 1p as a predictor of unfavorable outcome in patients with neuroblastoma. *N Engl J Med* 1996;**334**: 225–30.
8. Bown N, Cotterill S, Lastowska M, et al. Gain of chromosome arm 17q and adverse outcome in patients with neuroblastoma. *N Engl J Med* 1999;**340**:1954–61.
9. Cohn SL, Pearson ADJ, London WB, et al. The International Neuroblastoma Risk Group (INRG) Classification System: An INRG Task Force Report. *J Clin Oncol* 2009;**27**:289–97.
10. Cox DR. Regression models and life-tables. *J Royal Stat Soc (B)* 1972;**34**:187–220.
11. Machin D, Cheung Y-B, Parmar MKB. *Survival analysis: a practical approach*. Chichester: John Wiley; 2006.
12. Brodeur GM, Pritchard J, Berthold F, et al. Revisions of the international criteria for neuroblastoma diagnosis, staging, and response to treatment. *J Clin Oncol* 1993;**11**:1466–77.
13. Monclair T, Brodeur GM, Ambros PF, et al. The International Neuroblastoma Risk Group (INRG) Staging System. *J Clin Oncol* 2009;**27**:298–303.
14. StataCorp. Stata Statistical Software: Release 10.0. College Station. Texas: Stata Press; 2007.
15. London WB, Castleberry RP, Matthay KK, et al. Evidence for an age cutoff greater than 365 days for neuroblastoma risk group stratification in the Children's Oncology Group. *J Clin Oncol* 2005;**27**:6459–65.
16. Matthay KK, Villablanca JG, Seeger RC, et al. Treatment of high-risk neuroblastoma with intensive chemotherapy, radiotherapy, autologous BM transplantation, and 13-cis-retinoic acid. Children's Cancer Group. *N Engl J Med* 1999;**341**:1165–73.

Pediatr Blood Cancer 2011;56:865–867

BRIEF REPORT

Detection of *MYCN* DNA in the Cerebrospinal Fluid for Diagnosing Isolated Central Nervous System Relapse in Neuroblastoma

Tomiko Kimoto, MD,[1]* Masami Inoue, MD,[1] Sadao Tokimasa, MD, PhD,[1] Shigeki Yagyu, MD, PhD,[2] Tomoko Iehara, MD, PhD,[2] Hajime Hosoi, MD, PhD,[2] and Keisei Kawa, MD, PhD[1]

We present the case of a 1-year-old female with stage-4 neuroblastoma with *MYCN* amplification; she was treated with five chemotherapy courses, resulting in normalization of elevated serum levels of tumor markers. Complete remission was achieved after allogeneic hematopoietic stem-cell transplantation with reduced-intensity conditioning. Nine months later, however, the tumor relapsed in the central nervous system (CNS). The serum and cerebrospinal fluid (CSF) levels of the tumor markers were normal, but the *MYCN* copy number was high only in the CSF DNA, suggesting an isolated CNS recurrence. The *MYCN* copy number in the CSF DNA was reflective of response to treatment. Pediatr Blood Cancer 2011;56:865–867.

Key words: CNS relapse; *MYCN* DNA in the CSF; neuroblastoma,

INTRODUCTION

Neuroblastoma is the most common extracranial tumor of childhood. Metastatic disease is commonly found at its diagnosis. Although the frequency of spread of neuroblastoma to bone, bone marrow, and liver is high both at the initial diagnosis and at recurrence, metastasis to the central nervous system (CNS) is rare in terms of both brain parenchymal and leptomeningeal involvement. A recent study by the Children's Cancer Group (CCG) on metastatic sites in 567 patients with stage-4 neuroblastoma diagnosed between 1989 and 1996 revealed that only 0.7% and 2.2% of the patients had CNS involvement at diagnosis and at recurrence, respectively [1]. However, the improvement in the survival of children with metastatic neuroblastoma owing to recent advances in treatment has been accompanied by an increase in the frequency of CNS involvement [2,3].

MYCN amplification is strongly associated with rapid tumor progression and a poor outcome, independent of the stage of the tumor [4]. In addition, *MYCN* amplification is a significant risk factor for CNS relapse [3]. Reports have suggested that early recognition and aggressive treatment of this complication helps prevent tumor growth. Since the radiological features vary in each the patient [5,6], it is sometimes difficult to detect CNS relapse of neuroblastoma.

We report a case in which *MYCN* copy numbers in both serum and cerebrospinal fluid (CSF) samples were correlated with CNS neuroblastoma.

CASE REPORT

A 1-year-old female presented with proptosis and a left-sided abdominal mass. Computed tomography (CT) demonstrated a left adrenal mass (diameter, 4 cm; primary tumor) and cervical and celiac lymphadenopathy. Brain CT scan demonstrated soft tissue masses involving the skull. No areas of abnormal parenchymal or meningeal enhancements were visible, which indicated the absence of brain invasion. A lumber puncture was not performed at diagnosis. A primary tumor and generalized bone uptake were observed on meta-iodobenzylguanidine (MIBG) scanning; accordingly, stage-4 neuroblastoma was diagnosed. The tumor exhibited the unfavorable Shimada histology, with more than 40 *MYCN* copies, as evident on polymerase chain reaction (PCR) analysis. Tumor markers were abnormally elevated: the levels of urinary homovanillic acid (HVA) and serum neuron-specific enolase (NSE) were 145.24 μg/mg creatinine and 1,678 ng/ml, respectively. Complete remission was achieved after five courses of combination chemotherapy (regimen A1, comprising cyclophosphamide, vincristine, pirarubicin hydrochloride, and cisplatin) and resection of the primary tumor. The patient received allogeneic stem-cell transplantation from her human-leukocyte-antigen haplo-identical father after reduced-intensity conditioning, with melphalan and fludarabine, which was aimed at eliciting the graft-versus-tumor (GVT) response [7]. For prophylaxis against the graft-versus-host disease (GVHD), tacrolimus, and methotrexate were administered. The CD34 cell count was 4.4×10^6/kg and the nucleated cell count was 6.3×10^8/kg. Engraftment was confirmed by fluorescent in-situ hybridization on day 12. The patient developed GVHD grade III (skin, stage 3; gut, stage 3), which was controlled well by steroid administration. To induce a GVT effect, we attempted to wean this patient off the immunosuppressive drugs in a month. Four months after the stem-cell transplantation, the patient was admitted with altered consciousness [Glasgow coma scale: 3] and seizure associated with hydrocephalus. She also presented with paralysis of the lower extremities and a neuropathic bladder. A T1-weighted magnetic resonance (MR) image obtained at this time point showed extensive intraspinal pachymeningeal thickening and nodularity (Fig. 1). Tumor masses disturbed the flow of CSF. On the same day, ventriculo-peritoneal (V-P) shunt was implanted to decrease the pressure.

The new lesions were negative for MIBG uptake. Abdominal and pelvic CT did not reveal any other abnormalities. Diagnostic biopsy was not performed because of surgical risk. CSF was removed from the cranial end of the shunting system. The results of cytological analysis of the CSF were negative. Tumor markers were within the normal range: the levels of urinary HVA, serum NSE, CSF HVA, and

[1]Department of Hematology/Oncology, Osaka Medical Center and Research Institute for Maternal and Child Health, Osaka, Japan; [2]Department of Pediatrics, Kyoto Prefectural University of Medicine, Graduate School of Medicine, Kyoto, Japan

Conflict of interest: The authors declare no competing financial interests.

*Correspondence to: Tomiko Kimoto, Department of Hematology/Oncology Osaka Medical Center and Research Institute for Maternal and Child Health, 840 Murodo, Izumi City, Osaka 594-1101, Japan.
E-mail: tomiko@ifrec.osaka-u.ac.jp

Received 16 August 2010; Accepted 20 October 2010

DOI 10.1002/pbc.22925
Published online 16 January 2011 in Wiley Online Library (wileyonlinelibrary.com).

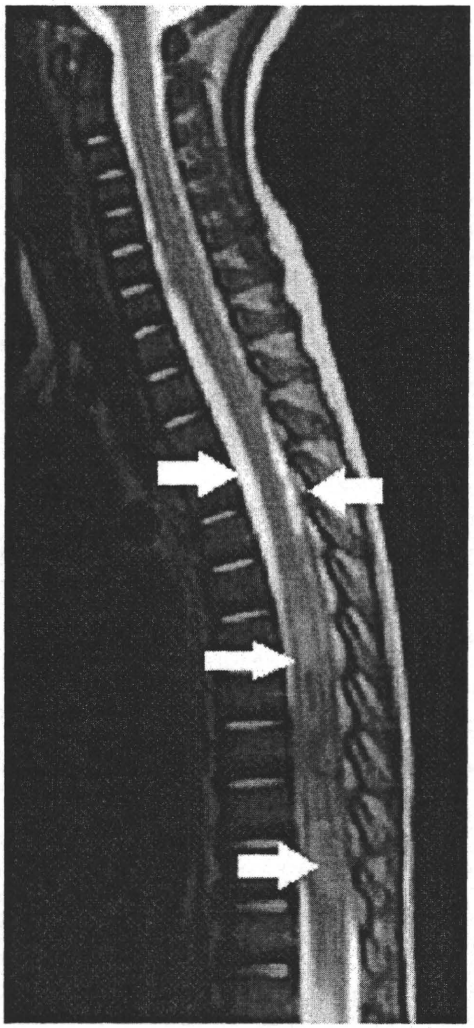

Fig. 1. Contrast-enhanced T1-weighted magnetic resonance image obtained during the first relapse shows an extensive intraspinal pachymeningeal thickening.

CSF NSE were 19.33 μg/ng creatinine, 14.4 ng/ml, 357 ng/ml (normal range: 322–520 ng/ml), and 111 ng/ml (indicating hemolysis), respectively. We measured the level of circulating *MYCN* DNA both in the CSF and serum, by using DNA-based real-time quantitative PCR with the *N*-acetylglucosamine kinase gene (*NAGK*, 2p12), The *MYCN* copy number was evaluated as previously described [8]. The *MYCN/NAGK* (M/N) ratio in the CSF sample obtained was 142.77, whereas that in the serum was 1.79, which was within the expected range. The clinical symptoms showed gradual improvement with repeated A1. Although, the contrast-enhancing masses of the spine remained, the CSF M/N ratio decreased to that in the serum (from 142.77 to 2.41). Seven months after the relapse, the patient complained of headache. CT scan revealed multiple masses in the brain, and she died from cerebral hemorrhage. The family did not permit post-mortem examination. The CSF M/N ratio increased from 2.41 to 12.09, while the serum M/N ratio and the other tumor markers were within the normal range (Fig. 2).

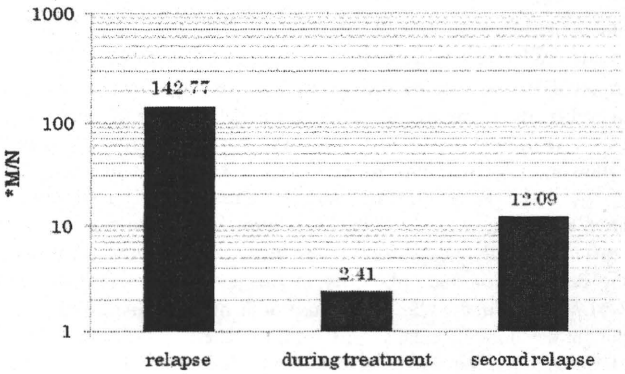

Fig. 2. The *MYCN/NAGK* (M/N) ratio in the CSF sample.

DISCUSSION

The prognosis of neuroblastoma with *MYCN* amplification is extremely poor. The long-term overall survival of patients with this tumor remains unsatisfactory (<40%) despite the improvement in the outcome by the use of intensive multimodal therapy with autologous hematopoietic stem-cell rescue. *MYCN* amplification is strongly associated with a poor prognosis, irrespective of age [9].

Molecular techniques such as PCR have enabled the detection of small amounts of free DNA in the serum and plasma of several cancer patients, and the level of free DNA is known to decrease when the patients respond to radiotherapy; this suggests that the level of free DNA can be considered as a valuable marker for cancer detection [10,11].

Combaret et al.[12] reported that high levels of *MYCN* DNA were present in the peripheral blood of patients with *MYCN*-amplified neuroblastoma (MNA).

However, the results of the assay for this DNA could be influenced by the quality of the template DNA or a numerical change in chromosome 2. Gotoh et al. [8] used DNA-based real time quantitative PCR and a single copy reference gene (*NAGK*) located on 2p12 for assessment of *MYCN*. *NAGK* is located on chromosome 2 but is distant from the region usually affected by changes in the number of *MYCN* copies of chromosome 2; therefore, the number of *MYCN* copies to the number of reference gene copies gives the *MYCN* copy number, even if there is a change in the number of copies of chromosome 2. Both the sensitivity and specificity of the serum M/N ratio as a diagnostic test were high in the above-mentioned study. In addition, Gotoh et al. reported that the serum M/N ratio was elevated even in patients having MNA with localized tumors. A quantitative method using serum DNA is not only a diagnostic tool for assessing MNA status, but serum DNA is also being considered an early marker in disease progression for monitoring patients with neuroblastoma [8,13].

The CNS is a rare site of neuroblastoma recurrence; however, with the increase in the survival of patients, CNS recurrence of tumors is being increasingly diagnosed. The CNS can serve as a sanctuary site for cancer cells, because the blood–brain barrier impedes the penetration of most chemotherapy agents. CNS involvement can be clinically occult and carries a poor prognosis. Predictive features at the time of diagnosis for CNS recurrence are patient age of 2–3 years, tumor *MYCN* amplification, and positive findings of CSF cytology [3]. High-risk patients with neuroblastoma should be monitored with appropriate modalities such as contrast-enhanced MRI of the brain

and spine to enable timely detection of CNS metastasis. Current treatments for CNS relapse are still inadequate. The MSKCC groups reported the potential to increase survival rates for patients with CNS neuroblastoma treated with compartmental intrathecal antibody-based radioimmunotherapy targeting minimal residual disease following surgery, craniospinal irradiation, and chemotherapy [14].

Our patient developed an isolated CNS relapse of neuroblastoma after allogeneic stem-cell transplantation. Although most of the conventional diagnostic techniques were only slightly useful for the detection of neuroblastoma in this case, the high level of *MYCN* copies in the CSF helped us confirm the relapse. When the patient developed a relapse of the tumor, the CSF M/N ratio was elevated, while the serum M/N ratio remained normal. These data suggest that tumors localized in the CNS could be overlooked if diagnostic assays based on serum DNA are used. The tumors in CNS may not release a significant amount of DNA into the systemic circulation. Our report suggests that the CSF M/N ratio may be an early tumor marker even if the tumor is isolated to the CNS. The finding seems to be important in the face of an increase in the number of deaths due to CNS recurrence of neuroblastoma. In similar cases, it will be imperative to confirm observation via tissue biology examination as well as our findings about the detection of *MYCN DNA*.

ACKNOWLEDGMENT

We thank the specialists in the Osaka Medical And Research Institute for Maternal and Child Health for treating the patient with us: Dr. Akihiro Yoneda (Department of Pediatric Surgery), Dr. Masahiro Nakayama (Department of Clinical Laboratory Medicine and Anatomic Pathology), Dr .Masanori Nishikawa (Department of Radiology), Dr. Jyunji Yamada, Dr. Osama Takemoto (Department of Neurosurgery).

REFERENCES

1. DuBois SG, Kalika Y, Lukens JN, et al. Metastatic sites in stage IV and IVS neuroblastoma correlate with age, tumor biology, and survival. Pediatr Hematol Oncol 1999;21:181–189.
2. Kramer K, Kushner B, Heller G, Cheung NK. Neuroblastoma metastatic to the central nervous system. The Memorial Sloan-Kettering Cancer Center experience and a literature review. Cancer 2001;91:1510–1519.
3. Matthay KK, Brisse H, Couanet D, et al. Central nervous system metastases in neuroblastoma: Radiologic, clinical, and biologic features in 23 patients. Cancer 2003;98:155–165.
4. Seeger RC, Brodeur GM, Sather H, et al. Association of multiple copies of the N-myc oncogene with rapid progression of neuroblastomas. N Engl J Med 1985;313:1111–1116.
5. Palasis S, Egelhoff JC, Morris JD, et al. Central nervous system relapse of treated stage IV neuroblastoma. Pediatr Radiol 1998;28:990–994.
6. Porto L, Kieslich M, Yan B, et al. Isolated CNS relapse in neuroblastoma. Neuropediatrics 2005;36:112–116.
7. Inoue M, Nakano T, Yoneda A, et al. Graft-versus-tumor effect in a patient with advanced neuroblastoma who received HLA haploidentical bone marrow transplantation. Bone Marrow Transplant 2003;32:103–106.
8. Gotoh T, Hosoi H, Iehara T, et al. Prediction of MYCN amplification in neuroblastoma using serum DNA and real-time quantitative polymerase chain reaction. J Clin Oncol 2005;23:5205–5210.
9. Matthay KK, Villablanca JG, Seeger RC, et al. Treatment of high-risk neuroblastoma with intensive chemotherapy, radiotherapy, autologous bone marrow transplantation, and 13-cis-retinoic acid. Children's Cancer Group. N Engl J Med 1999;341:1165–1173.
10. Leon SA, Shapiro B, Sklaroff DM, Yaros MJ. Free DNA in the serum of cancer patients and the effect of therapy. Cancer Res 1977;37:646–650.
11. Silva JM, Gemma Dominguez, Garcia JM, et al. Presence of tumor DNA in plasma of breast cancer patients clinicopathological correlations. Cancer Res 1999;59:3251–3256.
12. Combaret V, Audoynaud C, Iacono I, et al. Circulating MYCN DNA as a tumor-specific marker in neuroblastoma patients. Cancer Res 2002;62:3646–3648.
13. Combaret V, Hogarty MD, London WB, et al. Influence of neuroblastoma stage on serum-based detection of MYCN amplification. Pediatr Blood Cancer 2009;53:329–331.
14. Kramer K, Kushner BH, Modak S, et al. Compartmental intra thecal radioimmunotherapy: Results for treatment for metastatic CNS neuroblastoma. J Neurooncol 2010;97:409–418.

Pediatr Radiol (2010) 40:777–780
DOI 10.1007/s00247-009-1491-3

CASE REPORT

Unusual fatty metamorphosis observed in diffuse liver metastases of stage 4S neuroblastoma

Jun Tazoe · Chio Okuyama · Tomoko Iehara · Hajime Hosoi · Tsunehiko Nishimura

Received: 8 April 2009 / Revised: 9 August 2009 / Accepted: 1 November 2009 / Published online: 24 February 2010

Abstract We report a case of stage 4S neuroblastoma in which CT showed diffuse liver metastases containing a geographical fatty area in the periportal region. MRI showed this abnormality to correspond to an area with an unusual pattern of fatty change. ^{123}I-metaiodobenzylguanidine (MIBG) scintigraphy demonstrated increased accumulation throughout the liver, except for the region showing fatty change. To the best of our knowledge, this is the first report of liver metastases from neuroblastoma with geographical fatty infiltration.

Keywords Infantile neuroblastoma · Liver · Metastasis · ^{123}I-MIBG · MRI · Child

Introduction

Neuroblastoma (NB) is the most common malignant solid tumour of infancy and childhood. Age and initial stage are the important prognostic factors for this disease [1]. In the International NB Staging System, stage 4 encompasses all patients with distant disease, except a special category that is labelled stage 4S [2]. Stage 4S is defined as infants who have a small resectable primary tumour, with distant metastases restricted to the liver, bone marrow, or skin.

^{123}I-metaiodobenzylguanidine (MIBG) has high affinity for tumours derived from neural crest tissue, and is thought to be indispensable for staging and evaluation of response to therapy of NB [3]. Here, we report a case of stage 4S NB with diffuse liver metastases containing an atypical fatty area. In this case, MRI and ^{123}I-MIBG scintigraphy were helpful in the evaluation of the unusual liver finding demonstrated by CT.

J. Tazoe (✉) · C. Okuyama · T. Nishimura
Department of Radiology, Graduate School of Medical Science,
Kyoto Prefectural University of Medicine,
465 Kajiicho Kawaramachi Hirokoji Kamigyo-ku,
Kyoto City 602-8566, Japan
e-mail: juntazoe@gmail.com

T. Iehara · H. Hosoi
Department of Paediatrics, Graduate School of Medical Science,
Kyoto Prefectural University of Medicine,
465 Kajiicho Kawaramachi Hirokoji Kamigyo-ku,
Kyoto City 602-8566, Japan

Case report

A 3-month-old girl with abdominal distension was admitted to our hospital. She was born at 39 weeks' gestation and delivery and early postnatal period were uncomplicated. Her parents first noticed her abdominal distension at 1 month of age that gradually increased over time. Physical examination revealed tachycardia, tachypnoea and hepatomegaly. Her laboratory findings were: white blood cell count 14.8×10^9/l, haemoglobin 10.9 g/dl, platelets 45.7×10^4/μl, AST 103 IU/l, LDH 348 IU/l. Some tumour markers were elevated; serum neuron specific enolase (NSE) 110 ng/ml, urine vanillylmandelic acid (VMA)/creatinine (Cr) 1,938 mg/g Cr, urine homovanillic acid (HVA)/Cr 1,058 mg/g Cr, α-fetoprotein (AFP) 12,435 ng/ml. Bone marrow studies showed a clump of atypical tumour cells (5.8%) and revealed normal karyotype with no rearrangement or gene deletion or N-myc gene amplification.

Contrast-enhanced CT scan (Fig. 1) demonstrated marked hepatomegaly and a low-attenuation area in the periportal region with a geographically widespread distribution. Intrahepatic vessels seemed to pass through this area normally. A

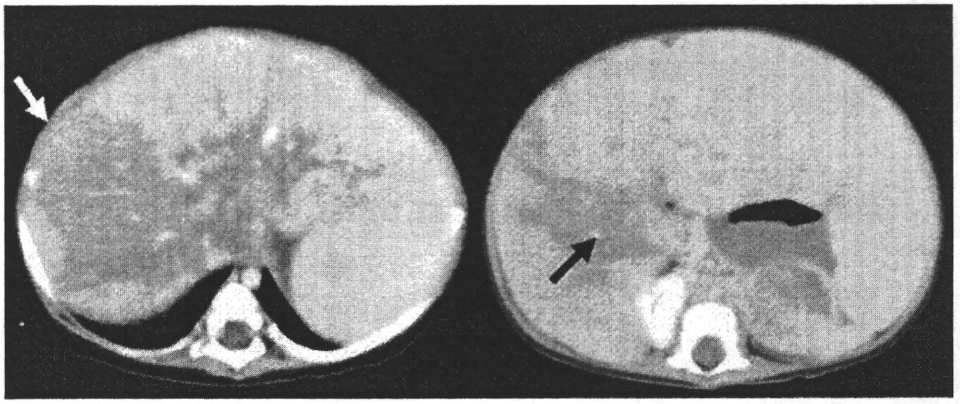

Fig. 1 Axial contrast-enhanced CT shows a geographically hypodense area in the periportal region (*white arrow*), in which the vascular architecture can be identified (*black arrow*)

heterogeneous mass was seen in the left adrenal grand. No enlarged lymph nodes were observed.

Abdominal MRI (Fig. 2) was performed for further evaluation. The area corresponding to the low-attenuation region on CT was hyperintense on T1-weighted (T1-W) in-phase images with decreasing signal on out-of-phase imaging and hypointense on superparamagnetic iron oxide (SPIO)-enhanced imaging. SPIO-enhanced imaging demonstrated hyperintense signal spread widely throughout the liver with sparing of the periportal region. Inhomogeneous nodular high signal was visualized on T2-weighted (T2-W) imaging. These findings indicate that the low-attenuation area represents fatty change with normal Kupffer cell function, while abnormal cells had infiltrated the remainder of the liver. The left adrenal mass had inhomogeneous high signal intensity on T2-W images with very intense signal in its centre suggesting cystic change.

^{123}I-MIBG scintigraphy (Fig. 3) was performed to confirm the diagnosis of NB and for staging. Intense accumulation was seen in the markedly enlarged liver. The periportal area with SPIO accumulation was photopenic on single photon emission CT (SPECT). Areas of

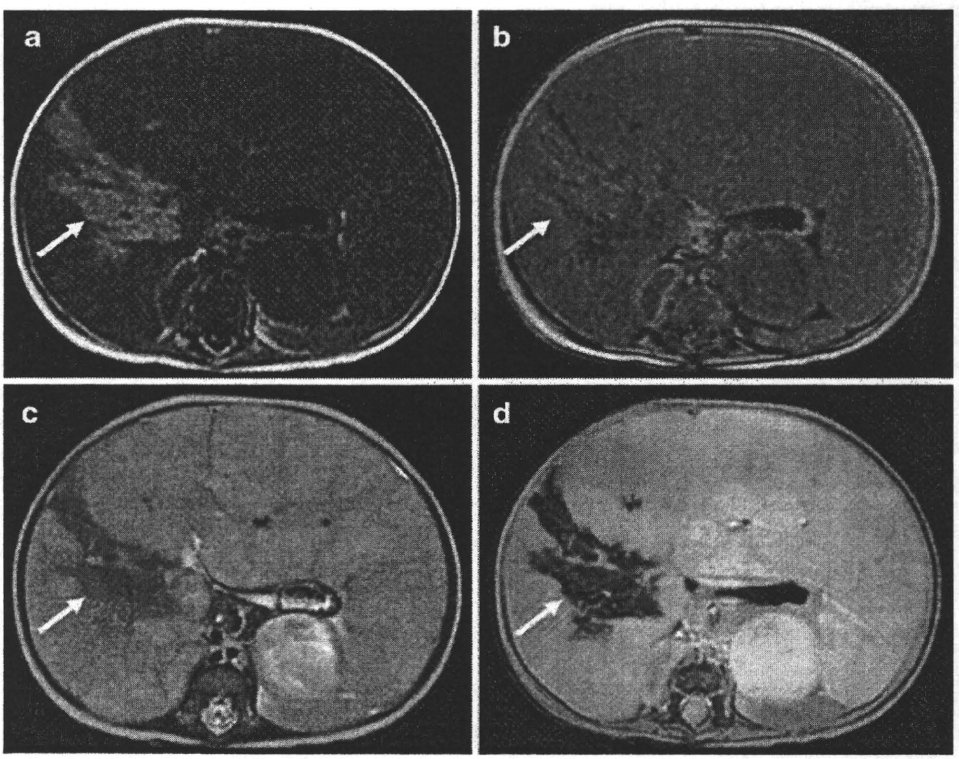

Fig. 2 Axial MRI. The periportal area is demonstrated as a fat-containing area by high signal on **a** T1-W in-phase and decreased signal on **b** T1-W out-of-phase images. Normal Kupffer cell function is shown by hypointense signal on **c** T2* SPIO-enhanced and **d** proton density-weighted SPIO images with surrounding diffusely abnormal areas without SPIO concentration (*arrows*)

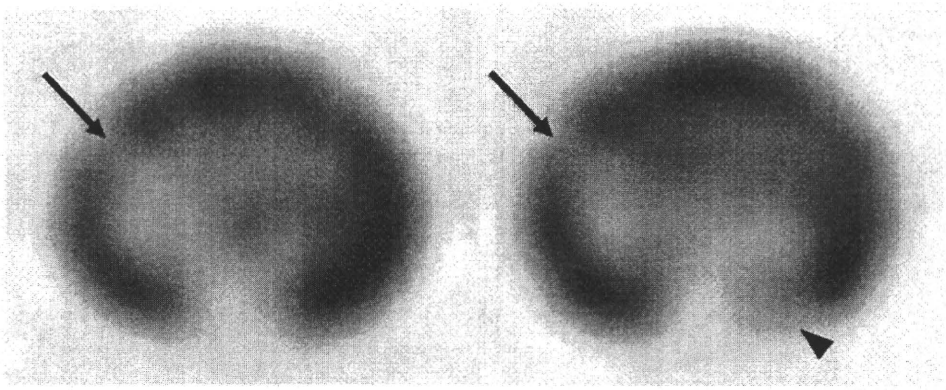

Fig. 3 ^{131}I-MIBG SPECT. Images shown correspond to the CT levels of Fig. 1. Intense accumulation of MIBG is seen in the periphery of the liver. The periportal region is shown as a photopenic area (*arrow*). Abnormal ring-like MIBG accumulation is seen in the cystic left adrenal mass (*arrowhead*)

doughnut-like abnormal accumulation were also seen in the cystic left adrenal gland mass. Bone marrow biopsy revealed infiltration of NB cells, and so the girl was diagnosed with left adrenal NB with liver and bone marrow metastases (stage 4S).

Since she had severe dyspnoea caused by the prominent hepatomegaly, radiotherapy was performed. When the dyspnoea had improved, chemotherapy was commenced. Four months later, the fatty area without MIBG accumulation increased in size, and the hyperintense area on T2-W images that showed MIBG accumulation became restricted to the periphery of the liver (Fig. 4). Following radiotherapy, six courses of chemotherapy and resection of the primary tumour, she is under observation.

Discussion

Approximately 80% of cases of stage 4S NB have liver metastases [4]. In previous reports, the morphological characteristics of the liver metastases were divided into two patterns; multiple nodular and diffuse infiltrative that spread throughout the liver [5]. Liver enlargement is frequently observed.

In our case, characteristic geographical fatty infiltration surrounding the porta hepatis was seen associated with diffuse tumour throughout the liver. SPIO-MRI and ^{123}I-MIBG scintigraphy were useful for the diagnosis of NB liver metastases, and revealed that the area of fatty change was spared from the surrounding diffuse tumour infiltration.

Stage 4S NB often disappears without treatment. The Ras gene is considered to work as a mediator of the programmed cell death system [6]. When tumour growth is more rapid than the natural death of tumour cells, marked liver enlargement causes dyspnoea and renal dysfunction resulting in early patient demise. However, some tumours vanish with no treatment (when natural death of the tumour cells is faster than tumour growth) and patients in this group have a good prognosis.

In the liver, SPIO particles are sequestered by reticuloendothelial Kupffer cells. Their superparamagnetic properties cause a shortening of the T2 time and subsequent decrease in the signal intensity of liver containing normal Kupffer cells. In this case, SPIO-MRI was useful to distinguish the fatty area from tumour infiltration. The periportal fatty area, with SPIO concentration and without high MIBG accumulation, surrounded by active NB is a unique and interesting finding in this case. However, we could not obtain pathological proof of this. The expansion of this area after treatment raises the possibility of it reflecting the natural regressive course of 4S tumour.

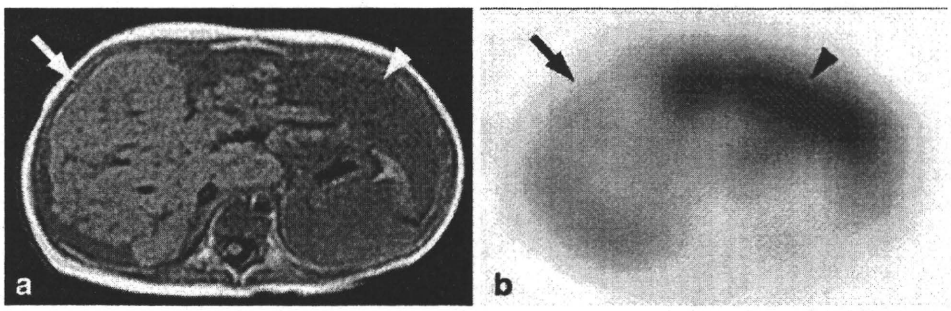

Fig. 4 Follow-up imaging 4 months after chemotherapy. **a** T1-W in-phase axial MRI and **b** MIBG SPECT. The liver has decreased in size and the fatty area without MIBG accumulation has expanded (*arrow*). The hypointense area with MIBG accumulation is restricted to the periphery of the liver (*arrowhead*)

References

1. Weinstein JL, Katzenstein HM, Cohn SL (2003) Advances in the diagnosis and treatment of neuroblastoma. Oncologist 8:278–292
2. Brodeur GM, Pritchard J, Berthold F et al (1993) Revisions of the international criteria for neuroblastoma diagnosis, staging, and response to treatment. J Clin Oncol 11:1466–1477
3. Shulkin BL, Shapiro B (1998) Current concepts on the diagnostic use of MIBG in children. J Nucl Med 39:679–688
4. Kushner BH, Kramer K, LaQuaglia MP et al (2006) Liver involvement in neuroblastoma: the Memorial Sloan-Kettering Experience supports treatment reduction in young patients. Pediatr Blood Cancer 46:278–284
5. Franken EA Jr, Smith WL, Cohen MD et al (1986) Hepatic imaging in stage IV-S neuroblastoma. Pediatr Radiol 16:107–109
6. Kitanaka C (2005) Non-apoptotic programmed cell deaths: existence and significance of programmed cell deaths having morphology and mechanism distinct from apoptosis. Yamagata Med J 23:83–96

ANTICANCER RESEARCH *30*: 3833-3838 (2010)

Optimal Cutoff Points of CYFRA21-1 for Survival Prediction in Non-small Cell Lung Cancer Patients Based on Running Statistical Analysis

HIDETO TAKAHASHI[1], KOICHI KURISHIMA[2], HIROICHI ISHIKAWA[3], KATSUNORI KAGOHASHI[4], MIO KAWAGUCHI[2] and HIROAKI SATOH[4]

[1]*Life System Medical Sciences, and* [2]*Division of Respiratory Medicine, Graduate School of Comprehensive Human Sciences, University of Tsukuba, Tsukuba, Ibaraki, Japan;*
[3]*Division of Respiratory Medicine, Tsukuba Medical Center Hospital, Tsukuba, Ibaraki, Japan;*
[4]*Division of Respiratory Medicine, Mito Medical Center, University of Tsukuba, Tsukuba, Ibaraki, Japan*

Abstract. *Purpose: To determine pretreatment serum CYFRA21-1 levels as indicators of poor prognosis in patients with non-small cell lung cancer (NSCLC). Methods: 1,202 consecutive patients, diagnosed pathologically with NSCLC from January 1999 to December 2009, were entered in this study. To obtain optimal cutoff points of CYFRA21-1 for these endpoints, a running log-rank statistical method was applied. Results: The cutoff level for the maximum log-rank statistical value of one-year survival in patients with NSCLC was 18.0 ng/ml. These results could be applied to patients with squamous cell carcinoma. In multivariate analysis, elevated (>18.0 ng/ml) levels of CYFRA21-1 was confirmed as being an unfavourable prognostic factor. Conclusion: CYFRA21-1 assay has a clinical significance for identifying patients with poor prognosis among those with early and advanced NSCLC. Elevated serum CYFRA21-1 levels at the time of diagnosis may be a useful noninvasive marker for identifying the risk of early death from NSCLC.*

Non-small cell lung cancer (NSCLC) accounts for 80% of all lung cancer cases, presenting as locally advanced in approximately 25-30% of cases and as metastatic disease in approximately 40-50% of cases. After radical treatment for seemingly localised disease, 20% of these patients develop an early distant relapse, probably due to systemic micrometastases that were present at the time of initial staging. One- and two-year survival rates are still used as the indices of survival for advanced NSCLC patients (1, 2).

Cytokeratin is a cytoskeletal structure expressed in epithelial cells, including bronchial epithelia (3). More than 20 subunits of cytokeratin are known and are expressed differently in several types of epithelia (4). Of these cytokeratins, cytokeratin 19 fragment (CYFRA21-1) levels in serum have already been evaluated as a useful tumour marker for non-small cell lung cancer (NSCLC) (5-18). Several studies have shown that elevated serum level of CYFRA21-1 is an independent prognostic factor of the risk of cancer death (8-18). The elevated serum levels of CYFRA21-1 could serve as a separate measure of biological aggressiveness and may have an important role in guiding treatment recommendations and in patient selection for clinical trials. However, regarding the use of CYFRA21-1 as a prognostic tool, neither the way of defining its cutoff points nor the use of multiple cutoff points for various survival conditions have been discussed in the published literature to date.

In evaluating the prognostic significance of elevated serum levels of CYFRA21-1, all the previous studies used manufacturer recommended cutoff levels of CYFRA21-1 for diagnosis of lung cancer (8-10, 12-18). Only one previous study analysed novel cutoff levels for poor prognosis (11). To calculate an optimal cutoff point, that study applied the receiver operation characteristic (ROC) method. This method, however, proved to be inapplicable because follow-up cases were not treated adequately in the survival analysis. In order to circumvent this weakness, a running log-rank statistic was calculated for each possible cutoff point on the basis of serum CYFRA21-1 level (19). The most optimal cutoff level was then determined as that corresponding to the maximum log-rank statistical value. As mentioned above, one- and two-year

Correspondence to: Hiroaki Satoh, MD, Division of Respiratory Medicine, Mito Medical Center, University of Tsukuba, Mito-city, Ibaraki, 310-0015, Japan. Tel: +81 292312371, e-mail: hirosato@md.tsukuba.ac.jp

Key Words: Non-small cell lung cancer, cytokeratin, tumour marker, CYFRA21-1, prognosis, survival.

0250-7005/2010 $2.00+.40

survival rates are still used as the index of the survival for advanced NSCLC patients (1, 2). This study evaluated the CYFRA21-1 level which attained the maximum log-rank statistical value of one-, two-, and three-year survival time.

Patients and Methods

Study population. A retrospective study of serum CYFRA21-1 levels was conducted in patients with NSCLC. 1,202 consecutive patients, diagnosed pathologically with NSCLC at the Divisions of Respiratory Medicine and Thoracic surgery, Tsukuba University Hospital and Division of Respiratory Medicine, Tsukuba Medical Center Hospital from January 1999 to December 2009, were entered in this study. Staging procedure was performed for all patients according to TNM classification (20) using chest computed tomography (CT), brain magnetic resonance imaging (MRI), bone scan as well as ultrasonograpy and/or CT of the abdomen. Peripheral venous blood samples collected from patients with NSCLC were used for the CYFRA21-1 assay. The samples were stored at –30°C until use. This study was approved by the Institutional Review Boards of the participating hospitals.

Measurement of CYFRA21-1 levels. Blood sampling was performed within the 1-month period preceding therapy. The serum CYFRA21-1 level of all blood samples was determined using a chemiluminescent enzyme immunoassay method (Lumipulse I CYFRA, Fujirebio Inc, Tokyo, Japan). According to the manufacturer, the upper limit of the normal CYFRA21-1 level is 3.5 ng/ml. The assay was performed by technicians who had no clinical information regarding the samples.

Statistical methods. To obtain optimal cutoff levels of CYFRA21-1, running log-rank statistics was applied (19). Running log-rank statistics produced for each cutoff point of serum level of CYFRA21-1 were plotted against survival and tested for statistical significance *via* permutations of the data. In brief, the patients were divided into two groups: patients with serum CYFRA21-1 levels more than the cutoff point and those with serum CYFRA21-1 levels equal to or less than the cutoff point. Log-rank statistical values between the groups were calculated for each possible cutoff point on the basis of serum CYFRA21-1 up to level that covered 90% of the patients by 1.0 ng/ml increments. The CYFRA21-1 level which attained the maximum log-rank statistical value of one-, two- and three-year survival time between the two groups was evaluated as an optimal cutoff point. All statistical analyses were performed using the SAS 9.1.3 for Windows and R (R-2.7.0) computer packages (Cary, North Carolina, USA). *p*-values less than 0.05 were considered to be statistically significant.

Results

Table I shows the basic characteristics of NSCLC patients. Of the 1,202 NSCLC patients, 906 were men. Median age was 68 years (range: 21-94 years). Among them were 280 stage *IA-IB* and 728 stage IIIB and IV. Histological types were: 733 patients with adenocarcinoma (AD), 399 with squamous cell carcinoma (SQ), 60 with large cell carcinoma, and 10 with other types as defined by the WHO classification system.

Table I. *Characteristics of patients with non-small cell lung cancer.*

No. of patients	1,202
Age (year)	median: 68 range: 21-94
Gender	
Male	906 (75.4%)
Female	296 (24.6%)
Performance status	
0-1	963 (80.2%)
2-4	238 (19.8%)
Histology	
Adenocarcinoma	733 (61.0%)
Squamous cell carcinoma	399 (33.2%)
Large cell carcinoma	60 (5.0%)
Other	10 (0.8%)
Clinical stage	
IA-B	280 (23.3%)
IIA-B	58 (4.8%)
IIIA	136 (11.3%)
IIIB	285 (27.7%)
IV	443 (36.9%)

The serum CYFRA21-1 levels differed significantly according to clinical stage (Kruskal-Wallis test, p=0.0001). Maximum serum level of CYFRA21-1 was 562.1 ng/ml, and CYFRA21-1 level up to 20.0 ng/ml covered 94.2% of all 1,202 NSCLC patients.

As shown in Figure 1, the maximum log-rank statistical value of one-year survival in patients with NSCLC was 0.455, which gave an optimal cutoff point for CYFRA21-1 level of 18.0 ng/ml. The maximum log-rank statistical value of two- and three-year survival in patients with NSCLC was 0.485 and 0.489, which gave optimal cutoff points of 3.0 ng/ml and 1.0 ng/ml, respectively. In patients with AD, the maximum log-rank statistical value of one-year survival was 0.531 which gave an optimal cutoff point of 5.0 ng/ml. The maximum log-rank statistical value of two- and three-year survival in patients with AD was 0.524 and 0.504 which gave optimal cutoff points of 5.0 ng/ml and 5.0 ng/ml, respectively. In patients with SQ, the maximum log-rank statistical value of one-year survival was 0.476 which gave an optimal cutoff point of 18.0 ng/ml (Figure 2). The maximum log-rank statistical value of two- and three-year survival in patients with SQ was 0.665 and 0.723 which gave optimal cutoff points 1.0 ng/ml and 1.0 ng/ml, respectively.

Confirmation of the above results was performed using uni- and multivariate analysis. Elevated CYFRA21-1 levels (>18.0 ng/ml) in NSCLC patients showed statistical significance in survival (p=0.001, for uni- and multi-variate analysis). Elevated CYFRA21-1 levels (>18.0 ng/ml) in patients with SQ also conferred a poor prognosis (p=0.001 for uni- and multivariate analysis; data not shown).

Table II. *Uni- and multivariate analyses of prognostic factors in patients with non-small cell lung cancer.*

Factor	Uni-variate analysis (log-rank test) *p*-Value	Multivariate analysis (Cox's proportional hazard model) Hazard ratio	95%CI	*p*-Value
Stage (IA-IIIA, IIIB-IV)	0.001	2.72	1.48-5.01	0.001
Smoking (smoker, non-smoker)	0.004	0.20	0.07-0.60	0.004
Performance status (0-1, 2-4)	0.001	2.43	1.43-4.14	0.001
CYFRA21-1 (≤18.0, >18.0 ng/ml)	0.001	2.02	1.14-3.58	0.001
Treatment (surgery, other)	0.001	1.59	0.81-3.12	0.175

95% CI: 95% Confidence interval.

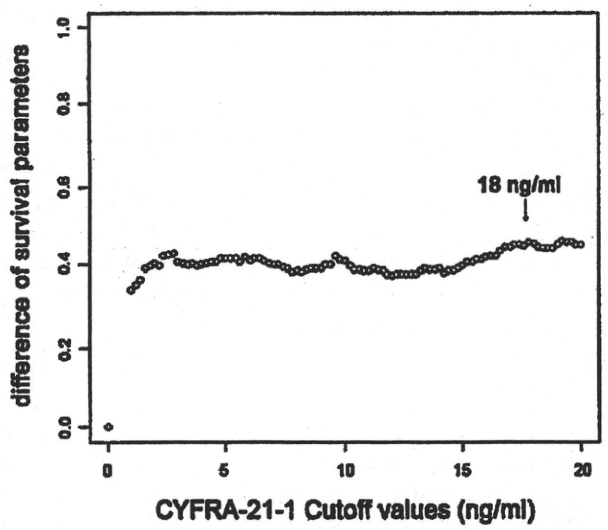

Figure 1. *Maximum log-rank statistical value of 1-year survival in patients with non-small cell lung cancer.*

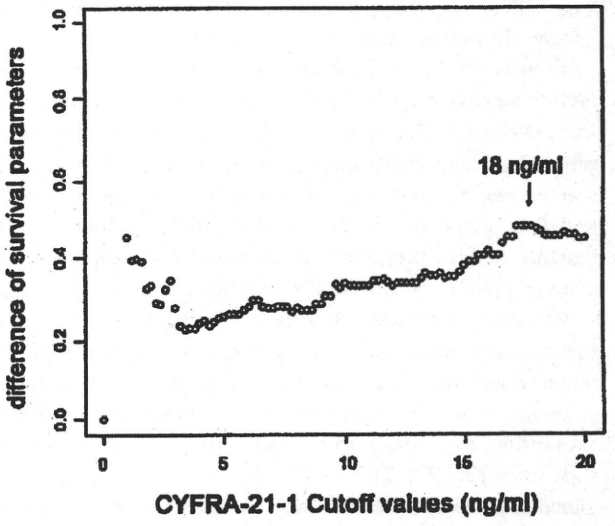

Figure 2. *Maximum log-rank statistical value of 1-year survival in patients with squamous cell carcinoma.*

Discussion

CYFRA21-1 is an immunometric assay measuring fragments of cytokeratin 19 and has been suggested to correlate with tumour burden and disease progression in NSCLC 12, 16). Prognostic significance of CYFRA21-1 has been discussed with conflicting results (5, 7, 11, 13, 14, 16-18). Most previous studies showed a prognostic significance for CYFRA21-1 (11, 13, 14, 16-18), while some studies did not (5, 7). In most of them, the prognostic significance of CYFRA21-1 was evaluated only for patients with resectable or resected NSCLC (9, 11, 18), or only for those with advanced disease (14, 17). In four large previous studies including more than one hundred NSCLC patients and which evaluated the prognostic significance of CYFRA21-1, the proportion of patients with early (stage IA-B) and advanced disease (stage IIIB-IV) was 8.7%-15.6%, and 62.7%-76.0%, respectively (6, 8, 10). However it would be preferable if the prognostic significance were evaluated in a large NSCLC patient population including both early and advanced clinical stages. Therefore, the present study evaluated serum CYFRA21-1 levels in NSCLC patients with operable stage as well as those with advanced or metastatic diseases. Above all, the major question dealt with in this study was whether patients who have elevated pretreatment serum CYFRA21-1 levels will have an unfavourable prognosis. If so, the next issue of this study was to determine pretreatment serum CYFRA21-1 levels that can be used as indicators of poor prognosis. Although currently the best predictor of outcome for patients with NSCLC is the TNM classification, the prognosis of patients within each stage of disease may vary considerably (1, 2). Early metastasis is a well-known feature of poor prognosis in potentially resectable NSCLC (21). The dissemination of malignant cells to distant organs *via* lymph nodes or blood vessels in NSCLCs can occur at an early stage of primary tumour growth and a significant number of early

staged NSCLC patients die of aggressive progression of the disease (21). In evaluating the prognostic significance of CYFRA21-1, most previous studies used the cutoff level that was recommended by the manufacturer of the assay kit, based on the specificity of the marker as the diagnostic tool to distinguish between lung cancer and normal individuals (8, 13-15). For example, Barlési *et al.* used a cutoff level of 3.5 ng/ml (14), and both Muley *et al.* and Merle *et al.* used a cutoff of 3.3 ng/ml (13, 15). In a large prospective study in 621 patients by Pujol *et al.*, the cutoff level was 3.6 ng/ml (10). Only Reinmuth *et al.* determined a cutoff CYFRA21-1 level using classification and regression tree survival analysis, resulting in a best predictive cutoff value of 3.57 ng/ml (11). The difference in the optimal CYFRA21-1 level for prognostic value between Reinmuth *et al.* (11) and the present study may be due to differences in the statistical analysis as well as the number of NSCLC patients and clinical stages of them evaluated. The analysis by Reinmuth *et al.* (11) included only 67 patients with completely resected NSCLC patients, and the proportion of stage IA-B and IIIB-IV cases were 85% and 0%, respectively. The present study included 1,202 patients, and the proportion of cases with early and advanced disease was 22.8% and 58.4%, respectively.

Recently, an optimal cutoff point for the diagnosis of lung cancer was determined using a ROC curve by choosing the value which attains the shortest length of (0, 1) point in the x-y plane, with the x axis representing the false positive proportion and the y axis representing the true positive proportion (22, 23). This method, however, does not cover the situation when censored data arise. To overcome this difficulty, running log-rank statistics (19) was applied in the present study. The value which attained the maximum statistic value between groups was naturally considered to be the best cutoff point for CYFRA2-1 levels. In this study, two notable results were found. Firstly, the maximum log-rank statistical value of one-year survival in NSCLC patients gave an optimal cutoff point of 18.0 ng/ml. The same cutoff level was also given by the maximum log-rank statistical value of one-year survival in SQ patients. Rather than the upper level for diagnosis, these findings could provide more important clinical information on identifying patients with poor prognosis. It seems reasonable that the optimal CYFRA21-1 point for poor prognosis, which was evaluated in this study, was higher than the manufacturer recommended cutoff value for diagnosis of NSCLC. Secondly, the cutoff levels for the maximum log-rank statistical value of two- and three-year survival in NSCLC, AD, and SQ patients were almost the same as the manufacturer recommended cutoff value for diagnosis. This result seemed to be somewhat unexpected; however, it may mean that if a patient had lung cancer with a higher CYFRA21-1 level than the manu-facturer recommended cutoff value, they would have a considerably unfavorable prognosis, irrespective of the histological type of NSCLC.

In spite of these significant findings, this study has limitations that need to be addressed before serum CYFRA21-1 can be used clinically at the time of diagnosis to predict subsequent mortality. Firstly, changes in serum CYFRA21-1 levels in serial measurement may be of great importance; however, this conclusion is only speculative, as there is no definite information on the serial measurements of CYFRA21-1 and changes in its level. Secondly, this study included NSCLC patients treated with various kinds of therapies. Thirdly, the development of these therapies may have influenced the prognosis of the patients. Therefore, these limitations may have affected the results of the present study.

In conclusion, elevated levels of CYFRA21-1 (>18.0 ng/ml) in NSCLC patients suggest a poor prognosis. In patients with SQ, CYFRA21-1 levels (>18.0 ng/ml) also predict poor prognosis. These findings suggest that CYFRA21-1 assay have a clinical significance for identifying patients with a poor prognosis among those with early and advanced NSCLC. In other words, elevated serum CYFRA21-1 levels at the time of diagnosis may be a useful noninvasive marker for identifying the risk of early death from NSCLC. A careful and large-sized clinical study may be necessary to corroborate these results.

References

1 Okamoto T, Maruyama R, Shoji F, Asoh H, Ikeda J, Miyamoto T, Nakamura T, Miyake T and Ichinose Y: Long-term survivors in stage IV non-small cell lung cancer. Lung Cancer *47*: 85-91, 2005.

2 Satoh H, Ishikawa H, Ohara G, Kagohashi K, Kurishima K, Ohtsuka M and Hizawa N: Long-term survivors after chemotherapy in advanced non-small cell lung cancer. Anticancer Res *27*: 4457-4460, 2007.

3 Coulombe PA: The cellular biology of keratins: beginning a new era. Curr Opin Cell Biol *5*: 17-29, 1993.

4 Iyonaga K, Miyajima M, Suga M, Saita N and Ando M: Alterations in cytokeratin expression by the alveolar lining epithelial cells in lung tissue from patients with idiopathic pulmonary fibrosis. J Pathol *182*: 217-224, 1997.

5 Niklinski J, Furman M, Chyczewska E, Chyczewski L, Rogowski F, Jaroszewicz E and Laudanski J: Evaluation of CYFRA 21-1 as a new marker for non-small cell lung cancer. Eur J Cancer Prev *3*: 227-230, 1994.

6 Wieskopf B, Demangeat C, Purohit A, Stenger R, Gries P, Kreisman H and Quoix E: Cyfra 21-1 as a biologic marker of non-small cell lung cancer. Evaluation of sensitivity, specificity, and prognostic role. Chest *108*: 163-169, 1995.

7 Szturmowicz M, Sakowicz A, Rudzinski P, Zych J, Wiatr E, Zaleska J and Rowinska-Zakrzewska E: The clinical value of Cyfra 21-1 estimation for lung cancer patients. Int J Biol Markers *11*: 172-177, 1996.

8 Bréchot JM, Chevret S, Nataf J, Le Gall C, Frétault J, Rochemaure J and Chastang C: Diagnostic and prognostic value of Cyfra 21-1 compared with other tumour markers in patients with non-small cell lung cancer: a prospective study of 116 patients. Eur J Cancer *33*: 385-391, 1997.

9 Niklinski J, Burzykowski T, Niklinska W, Laudanski J, Chyczewski L, Rapellino M and Furman M: Preoperative CYFRA 21-1 level as a prognostic indicator in resected nonsmall cell lung cancer. Eur Respir J *12*: 1424-1428, 1998.
10 Pujol JL, Boher JM, Grenier J and Quantin X: Cyfra 21-1, neuron specific enolase and prognosis of non-small cell lung cancer: prospective study in 621 patients. Lung Cancer *31*: 221-231, 2001.
11 Reinmuth N, Brandt B, Semik M, Kunze WP, Achatzy R, Scheld HH, Broermann P, Berdel WE, Macha HN and Thomas M: Prognostic impact of CYFRA21-1 and other serum markers in completely resected non-small cell lung cancer. Lung Cancer *36*: 265-270, 2002.
12 Kulpa J, Wójcik E, Reinfuss M and Kołodziejski L: Carcinoembryonic antigen, squamous cell carcinoma antigen, CYFRA 21-1, and neuron-specific enolase in squamous cell lung cancer patients. Clin Chem *48*: 1931-1937, 2002.
13 Muley T, Dienemann H and Ebert W: Increased CYFRA 21-1 and CEA levels are negative predictors of outcome in *p*-stage I NSCLC. Anticancer Res *23*: 4085-4093, 2003.
14 Barlési F, Gimenez C, Torre JP, Doddoli C, Mancini J, Greillier L, Roux F and Kleisbauer JP: Prognostic value of combination of CYFRA21-1, CEA and NSE in patients with advanced non-small cell lung cancer. Respir Med *98*: 357-362, 2004.
15 Merle P, Janicot H, Filaire M, Roux D, Bailly C, Vincent C, Gachon F, Tchirkov A, Kwiatkowski F, Naamé A, Escande G, Caillaud D and Verrelle P: Early CYFRA 21-1 variation predicts tumor response to chemotherapy and survival in locally advanced non-small cell lung cancer patients. Int J Biol Markers *19*: 310-315, 2004.
16 Pujol JL, Molinier O, Ebert W, Daurès JP, Barlesi F, Buccheri G, Paesmans M, Quoix E, Moro-Sibilot D, Szturmowicz M, Bréchot JM, Muley T and Grenier J: CYFRA 21-1 is a prognostic determinant in non-small-cell lung cancer: results of a meta-analysis in 2063 patients. Br J Cancer *90*: 2097-2105, 2004.
17 Ardizzoni A, Cafferata MA, Tiseo M, Filiberti R, Marroni P, Grossi F and Paganuzzi M: Decline in serum carcinoembryonic antigen and cytokeratin 19 fragment during chemotherapy predicts objective response and survival in patients with advanced non-small cell lung cancer. Cancer *107*: 2842-2849, 2006.
18 Suzuki H, Ishikawa S, Satoh H, Ishikawa H, Sakai M, Yamamoto T, Onizuka M and Sakakibara Y: Preoperative CYFRA 21-1 levels as a prognostic factor in c-stage I non-small cell lung cancer. Eur J Cardiothorac Surg *32*: 648-652, 2007.
19 Crowley J, LeBlanc M, Jacobson J and Salmon S: Some exploratory tools for survival analysis. *In*: Lecture Notes on Statistics. Proceedings of the First Seattle Symposium in Biostatistics: Survival Analysis. New York: Springer, 199-229, 1997.
20 Mountain CF: Revisions in the international system for staging lung cancer. Chest *111*: 1710-1717, 1997.
21 Passlick B: Micrometastases in non-small cell lung cancer (NSCLC). Lung Cancer *34(Suppl 3)*: S25-9, 2001.
22 Ohara G, Satoh H and Hizawa N: Prognostic markers for stage I non-small cell lung cancer. Lung Cancer *59*: 137, 2008.
23 Satoh H, Ishikawa H, Kurishima K, Yamashita YT, Ohtsuka M and Sekizawa K: Cut-off levels of NSE to differentiate SCLC from NSCLC. Oncol Rep *9*: 581-583, 2002.

Received May 7, 2010
Revised June 4, 2010
Accepted June 9, 2010

Oncogene (2011) 30, 97–105

www.nature.com/onc

ORIGINAL ARTICLE

CD133 suppresses neuroblastoma cell differentiation via signal pathway modification

H Takenobu[1], O Shimozato[2], T Nakamura[3], H Ochiai[1,4], Y Yamaguchi[1], M Ohira[5], A Nakagawara[6] and T Kamijo[1]

[1]Division of Biochemistry and Molecular Carcinogenesis, Chiba Cancer Center Research Institute, Chiba, Japan; [2]Laboratory of Anti-tumor Research, Chiba Cancer Center Research Institute, Chiba, Japan; [3]Core Facility for Therapeutic Vectors, The Institute of Medical Science, The University of Tokyo, Tokyo, Japan; [4]Department of Pediatrics, Graduate School of Medicine, Chiba University, Chiba, Japan; [5]Laboratory of Cancer Genomics, Chiba Cancer Center Research Institute, Chiba, Japan and [6]Division of Biochemistry and Innovative Cancer Therapeutics, Chiba Cancer Center Research Institute, Chiba, Japan

CD133 (prominin-1) is a transmembrane glycoprotein expressed on the surface of normal and cancer stem cells (tumor-initiating cells), progenitor cells, rod photoreceptor cells and a variety of epithelial cells. Although CD133 is widely used as a marker of various somatic and putative cancer stem cells, its contribution to the fundamental properties of cancer cells, such as tumorigenesis and differentiation, remains to be elucidated. In the present report, we found that CD133 was expressed in several neuroblastoma (NB) cell lines/tumor samples. Intriguingly, CD133 repressed NB cell differentiation, for example neurite extension and the expression of differentiation marker proteins, and was decreased by several differentiation stimuli, but accelerated cell proliferation, anchorage-independent colony formation and *in vivo* tumor formation of NB cells. NB cell line and primary tumor-sphere experiments indicated that the molecular mechanism of CD133-related differentiation suppression in NB was in part dependent on neurotrophic receptor RET tyrosine kinase regulation. RET transcription was suppressed by CD133 in NB cells and glial cell line-derived neurotrophic factor treatment failed to induce RET in CD133-expressing cells; RET overexpression rescued CD133-related inhibition of neurite elongation. Of note, CD133-related NB cell differentiation and RET repression were mainly dependent on p38MAPK and PI3K/Akt pathways. Furthermore, CD133 has a function in growth and RET expression in NB cell line- and primary tumor cell-derived tumor spheres. To the best of our knowledge, this is the first report of the function of CD133 in cancer cells and our findings may be applied to improve differentiation induction therapy for NB patients.
Oncogene (2011) **30,** 97–105; doi:10.1038/onc.2010.383; published online 6 September 2010

Keywords: CD133; neuroblastoma; differentiation; RET p38MAPK; PI3K/Akt

Correspondence: Professor T Kamijo, Division of Biochemistry and Molecular Carcinogenesis, Chiba Cancer Center Research Institute, 666-2 Nitona, Chuo-ku, Chiba 260-8717, Japan.
E-mail: tkamijo@chiba-cc.jp
Received 2 March 2010; revised 5 July 2010; accepted 14 July 2010; published online 6 September 2010

Introduction

CD133 (AC133; human prominin-1) belongs to a family of cell-surface glycoproteins harboring five transmembrane domains (Corbeil *et al.*, 2001) and was originally found as a hematopoietic stem cell marker (Yin *et al.*, 1997). CD133 was subsequently shown to be expressed by a number of progenitor cells, including those of the epithelium, where it is expressed on the apical surface (Corbeil *et al.*, 2000). Previously, it was found that CD133-expressing cells in brain tumors have the capacity for unlimited self-renewal, as well as the ability, in small numbers, to initiate tumor formation and progression in immuno-deficient mice (Singh *et al.*, 2004), suggesting that CD133-expressing cells satisfy the important criteria required for tumor-initiating cells (TICs) (Reya *et al.*, 2001; Jordan *et al.*, 2006). Using similar methods, CD133 has recently been designated as a marker associated with TICs in the colon (O'Brien *et al.*, 2007; Ricci-Vitiani *et al.*, 2007), pancreatic (Olempska *et al.*, 2007), liver (Yin *et al.*, 2007), skin (Monzani *et al.*, 2007) and prostate (Collins *et al.*, 2005; Miki *et al.*, 2007) cancers. Maw *et al.* (2000) reported homozygosity for a 1-bp deletion (1878delG) in exon 16 of the CD133 gene predicted to cause a frameshift at codon 614 and a prematurely truncated protein lacking about half of the second extracellular loop, the final membrane-spanning segment and the cytoplasmic-C-terminal domain; this missense mutation caused retinal degeneration in four affected members of a consanguineous Indian family. This finding was further confirmed by an article describing that loss of Prom-1 in genetically modified mouse results in the progressive degeneration of mature photoreceptors with complete loss of vision (Zacchigna *et al.*, 2009); however, to the best of our knowledge, no reports have studied the function of CD133 in tumorigenesis.

Neuroblastoma (NB) is the most common pediatric solid malignant tumor derived from the sympathetic nervous system. Unlike the many childhood malignancies for which survival has been improved by recent therapies, high-risk NB is still one of the most difficult tumors to cure, with only 30% long-term survival despite intensive multimodal therapy (Maris *et al.*,

2007). The clinical presentation and treatment response of advanced NB, which results in relapse and a refractory state after a good responsive to the initial chemotherapy, suggest that TICs likely exist in NB tumors. A previous report indicated the isolation and characterization of putative TICs using primary-sphere formation with tumors and bone marrow metastases from NB patients, although CD133 expression was not detected in a bone marrow-derived high-risk NB tumorsphere sample (Hansford *et al.*, 2007). On the other hand, it was reported that sub-cloned NB cells (designated 'intermediate type'), which have a significantly more malignant phenotype, with four- to fivefold greater plating efficiencies in soft agar and sixfold higher tumorigenicity in athymic mice, expressed high amounts of CD133 mRNA compared with less malignant subclones (Walton *et al.*, 2004); therefore, the function of CD133 in NB tumorigenesis and aggressiveness remains unresolved.

Previous reports about CD133 expression in NB and its function as a stem cell marker in several tumors prompted us to study the function of CD133 in NB cells (Walton *et al.*, 2004; Hansford *et al.*, 2007). Our results clearly indicated that CD133 also seems to regulate cell proliferation and tumorigenesis in NB cells. Importantly, CD133 represses NB cell differentiation and is decreased by several differentiation stimulators. We studied the molecular mechanism of CD133-related differentiation inhibition in NB cells and found that it was in part dependent on RET tyrosine kinase receptor regulation via signal pathway modification. Furthermore, CD133 is expressed in NB cell spheres and has a function in sphere growth and RET regulation.

In specific malignancies, for example NB and acute promyelocytic leukemia, differentiation induction therapy using retinoic acid is clearly effective. *In vitro* experiments indicated that all-*trans*-retinoic acid (ATRA) treatment induced morphological and biochemical differentiation in these cancer cells, suggesting that the induced differentiation seems to repress the tumorigenic activity of cancer cells (Brodeur *et al.*, 2000; Weinberg, 2006). Together, CD133 may regulate NB tumorigenesis and proliferation by preventing differentiation.

Results

CD133 has a function in NB cell proliferation

First, we checked the expression of CD133 in NB cell lines and found its expression in 7 out of 20 (53%) cell lines (Figure 3d and Supplementary Figure 1S). A high level of cell-surface expression of *CD133* was detected in TGW and SK-N-DZ cells, and modest expression was found in IMR32 (Figure 1a; Supplementary Figure 1Sa). Next, we knocked down *CD133* in highly expressing NB cells and analyzed the knockdown-induced phenotype. Figure 1b shows that infection of shRNA-reduced CD133 mRNA and protein and *CD133* knockdown in TGW cells effectively resulted in significant growth retardation. Inhibition of cell proliferation by CD133 small-interference RNA was also observed in SK-N-DZ cells (Supplementary Figure S1). Furthermore, stable knockdown of *CD133* in TGW cells suppressed cell proliferation under anchorage-independent conditions (Figure 1c). To test tumorigenicity *in vivo*, *CD133*-silenced TGW cells were injected subcutaneously into nude mice. Mock shRNA lentivirus-infected cells formed large tumors within 9 days post-injection; CD133 shRNA lentivirus-infected cells formed very small tumors (Figure 1d). Next, we examined the effect of CD133 on NB cell proliferation (Supplementary Figure 2S). CD133 was successfully expressed in SH-SY5Y cells by lentivirus. The proliferation rate of CD133-expressing SH-SY5Y cells was 2–2.5-fold greater than mock cells. Moreover, a soft agar colony formation assay showed that CD133-expressing cells formed more and bigger colonies than mock-control cells.

CD133 knockdown induces NB differentiation

In NB cells, differentiation into a neuronal phenotype is induced when cells are treated with several stimulations. Glial cell line-derived neurotrophic factor (GDNF) induced neurite outgrowth in TGW cells (Figure 2a, center). In CD133 knocked-down TGW cells, neurite formation was observed even under normal culture conditions (Figure 2a, KD). We scored cells with neurite length longer than the cell body diameter as neurite positive (Figure 2b). CD133 knocked-down cells showed intensified neurite extensions when compared with mock cells. Mock-infected and CD133 knocked-down cells were collected at the end of the experiment, and mRNA was extracted and subjected to RT–PCR (Figure 2c). With *GAP43/neurofilament (NF) 68* as neuronal differentiation markers, these expressions were constitutively upregulated in CD133 knocked-down cells. Along with differentiation induced by treatment with ATRA or phorbol-12-myristate-13-acetate (TPA) in parental TGW cells, CD133 expression was suppressed at both protein and mRNA levels (Supplementary Figure 3S). These results indicated that CD133 may suppress the differentiation of NB cells.

CD133 regulates RET expression in NB cells

To identify the mechanism of CD133-related cellular differentiation, we studied the expression of several neurotrophic receptors and RET receptors because they are the important signal transduction pathway molecules, which have important functions in sympathetic nerve and NB cell differentiation (Kaplan *et al.*, 1993; Klein, 1994; D'Alessio *et al.*, 1995; Enomoto *et al.*, 2001). We introduced *CD133* cDNA into several NB cell lines (Figure 3a), and checked the effect of CD133 overexpression on *RET* expression using a primer pair recognizing all *RET* isoforms, *RET51*, *RET9* and *RET43*, formed by alternative splicing of C-terminal exon cassettes (Myers *et al.*, 1995; Enomoto *et al.*, 2000). Intriguingly, in *RET* and all *RET* isoforms, transcriptions were suppressed in CD133-overexpressing NB cells (*RET* reduction was 1.3–3.8-fold by qPCR); however,